

# Impact of daytime precipitation duration on urban heat island intensity over Beijing city

Ping Yang<sup>a,b,c</sup>, Guoyu Ren<sup>d,\*</sup>, Wei Hou<sup>e</sup>

<sup>a</sup> China Meteorological Administration (CMA) Training Center, Beijing, China

<sup>b</sup> Department of Atmospheric Science, School of Environmental Studies, China University of Geosciences, Wuhan, China

<sup>c</sup> Institute of Urban Meteorology CMA, Beijing, China

<sup>d</sup> Laboratory for Climate Studies, National Climate Center, CMA, Beijing, China

<sup>e</sup> National Climate Center, CMA, Beijing, China



## ARTICLE INFO

### Keywords:

Daytime  
Precipitation  
Duration  
UHI  
Diurnal variation  
Beijing city

## ABSTRACT

This study used the daytime hourly precipitation records and divided them into four types of duration to examine the impact of different daytime precipitation conditions on Urban Heat Island Intensity (UHII) over Beijing city. Results show that the magnitude differences of UHII are in close relation with the length of Continuous Precipitation Hours of Daytime (CPHD). The longer the CPHD, the less obvious the average UHI. When continuous precipitation events dominate the daytime, the diurnal variation pattern of UHII will be changed greatly. There are generally two (strong and weak) stable stages of UHII in no-rainy condition, while it disappears completely in the longest continuous daytime precipitation conditions. However, the diurnal cycles of UHII differences between each of the rainy daytimes and no-rain daytimes appear similar, with all of the dual peaks of the UHII differences occurring around sunrise (0600-0700 LST) and sunset (2000 LST), and the minimum of the UHII differences appearing stably from 1100 to 1500 LST.

## 1. Introduction

The previous studies have confirmed that urbanization has significant impacts on local to regional climate through land use and land cover transformations at the surface (Landsberg, 1981; Oke, 1988). Radical change in land use and land cover modifies the energy balance and boundary layer properties significantly, and is capable of inducing some unique climatic phenomena in cities, such as urban heat island (UHI) (Arnfield, 2003), urban rain island (Yang et al., 2017a) and urban dryness island (Yang et al., 2017b). Besides the influence of urbanization, the local climate phenomena surely depends on the geography and background atmospheric circulation. For example, land cover and availability of soil moisture make a significant contribution to the eventual positive or negative sign of the UHI (Georgescu et al., 2011). Recent work has specified the footprint effect of the built environment for surface temperature UHI of 32 cities across China based on MODIS land surface temperature data (Zhou et al., 2015).

As an important factor, weather condition is also strongly related to UHI effect. High pressure system in summer can restrain the development of a boundary layer, being conducive to UHI (Craig and Bornstein, 2002; Stewart and Oke, 2012). The steady weather system such as bright, calm, unclouded condition can help in developing strong UHI effect, while unstable weather will reduce the UHI effect (Landsberg, 1981; Oke, 1988). A number of studies have revealed significant correlation between UHII and cloudiness or

\* Corresponding author.

E-mail address: [guoyoo@cma.gov.cn](mailto:guoyoo@cma.gov.cn) (G. Ren).

<https://doi.org/10.1016/j.uclim.2019.100463>

Received 13 August 2017; Received in revised form 31 December 2018; Accepted 5 April 2019  
2212-0955/ © 2019 Elsevier B.V. All rights reserved.

solar radiation (Kim and Baik, 2002; Petralli et al., 2009; Arnds et al., 2017). It has also been demonstrated that UHII tends to be stronger at night, while becomes negative under moist conditions and larger thermal admittances by rural areas (Tereshchenko and Filonov, 2001; Yang et al., 2013c). Aerosols are another impact factor for UHII, because the presence of aerosols in urban environment could acts as clouds in the thermal equilibrium of urban boundary, and also affect the development of clouds and precipitation (Diem and Brown, 2004; Shimadera et al., 2015).

Precipitation is closely related to many other weather conditions including air temperature and atmospheric humidity. Continuous attentions have been paid to the possible linkage between UHI and precipitation over the last decades.

Previous studies have demonstrated that UHI effect has a significant impact on mesoscale circulation, resulting in abnormal convection and precipitation over urban areas (Changnon, 1979; Huff, 1986; Han et al., 2014; Zhong et al., 2015). Researches indicated that larger roughness in urban areas can enhance convection and precipitation (e.g. Thielen et al., 2000), while other researchers reported that the larger roughness could increase the convergence on the windward side of city (e.g. Rozoff et al., 2003). Recent simulation results appear to explain the physical mechanism behind observed increases of precipitation within the highly populated metropolitan area (Magaña et al., 2003; Benson-Lira et al., 2016).

However, most of previous studies on relationship between UHI and precipitation were focused on the UHI impact on precipitation event (e.g. Changnon et al., 1991; Aws et al., 2017; Yang et al., 2017a; Wang et al., 2019), and fewer works were made to examine the impact of precipitation on UHII. Some analyses have concluded that the UHII reduced with an increase in precipitation amount (Guo et al., 2009; Wang et al., 2009; Liu, 2014), but another analysis shows that the UHII will be reinforced in the region with higher annual precipitation (Zhao et al., 2014). In spite of the previous works, the roles of precipitation in modifying detailed pattern of UHII over urban areas still need further investigation.

Beijing is a mega city of mainland China, with > 15 million populations settling in the built-up areas. Due to the large and rapid change of urban environment, more intense UHI and precipitation in urban areas over Beijing have been observed in previous observational researches (Li et al., 2008; Miao et al., 2010; Song et al., 2014; Yang et al., 2017c). The strongest UHII generally appeared within or around the 4th Ring Road in Beijing City, in accordance to Beijing's major transportation system with a multi Ring-Road network (Yang et al., 2013c), and short-duration intense precipitation events dominate summer precipitation in urban regions of Beijing (Yang et al., 2013b, 2017c). The previous works on UHII and urban precipitation are independently conducted, and the association between them, in particular, the possible influence of daytime precipitation on UHII pattern, has not yet exclusively examined. The reason for the lack of thus studies may be because of the lack of denser and high-quality observational data in urban areas, which is a necessity for investigating the relations between UHI and precipitation events in a finer spatial and temporal scale.

The purpose of this paper is to examine how the UHII changes under different daytime precipitation conditions in Beijing urban areas. The UHII contrast between the no-rainy case and each of the rainy cases are analyzed by using hourly observational data of Automatic Weather Stations (AWS). It is well known that daytime solar radiation is one of the most important elements which could change the energy and water balances in urban surface, affecting the potency of diurnal UHII critically. Thus, the main emphasis of our research in this paper is to examine the possible impact of varied duration daytime precipitation (from 0400 LST to 2000 LST) on UHII. The analysis results would be helpful to further separate the driving force on UHI and to understand the formation mechanism of UHI.

## 2. Study area, data and methods

### 2.1. Study area

Beijing, a high-density mega city covering about 1.6 million square kilometers, is at the northern end of the North China Plain and in the south to the Yanshan Mountains. The flat southeast area occupies about 38% of Beijing, the elevations of which are roughly ranging from 20 m ASL (above sea level) to 80 m ASL. The northwest is mainly mountainous areas. Climatologically, Beijing has a typical monsoon-driven semi-humid to humid continental climate, which is hot and humid in summer and cold and dry in winter. The rainy days and precipitation amount in Beijing are mainly concentrated in summer (Jun-Jul-Aug), contributing to about two thirds of its annual total precipitation (Yang et al., 2017c).

With accelerating urban expansion, population in Beijing City undergoes a rapid growth and over half of the population settled in the urban areas. A multi Ring-Road (RR) system of transportation (including 4th, 5th and 6th RRs, Fig. 1) has been built in the urban regions so far (Yang et al., 2013c). The zones inside different RRs could represent different levels of urbanization with varied densities of city population and buildings as well. In this paper, stations located inside the 6th RR in Beijing are considered as the urban sites (Fig. 1).

### 2.2. Observational data

In this study, the observed hourly surface air temperature (1.5 m) and precipitation amount data from 65 stations in urban area of Beijing for time period 2007–2015 are obtained from the Meteorological Information Center, Beijing Meteorological Bureau (MIC/BMB). The data have been preliminarily quality-controlled by the MIC, and the possibly wrong records have been taken out by applying a regionally climatological extreme value method.

In order to increase the reliability of the analysis, the data are checked and quality-controlled once again using the methods by Yang et al. (2011) and Yang and Liu (2013). The incredible stations with unrepresentative observational environment have been taken out of the dataset, and the methods of threshold values and manual identification are applied in checking. Based on the

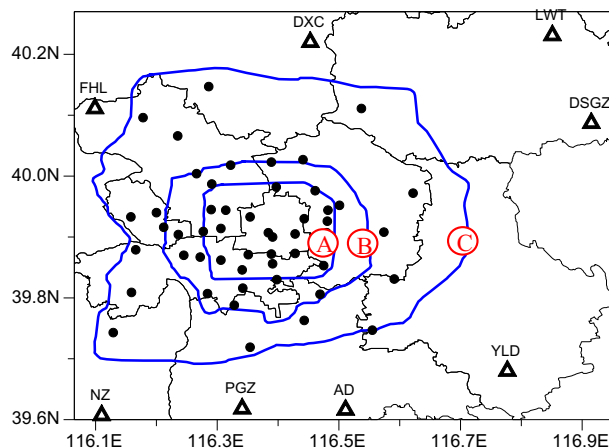


**Fig. 1.** Stations used in the Beijing urban region as outlined by the 6th Ring Road (blue solid circles, line A-C respectively represents 4th RR, 5th RR and 6th RR) and the 8 rural stations outside of the 6th Ring Road (Abbreviations of the station names are FHL for Feng Huang Ling, YLD for Yong Le Dian, PGZ for Pang Ge Zhuang, AD for An Ding, NZ for Nan Zhao, DSGZ for Da Sun Ge Zhuang, and LWT for Long Wan Tun , DXC for Dong Xin Cheng). (For interpretation of the references to colour in this figure legend, the reader is referred to the web version of this article.)

observational records and the climatological features in Beijing, different seasons have been given different threshold values for quality control both for temperature and precipitation data. If the hourly records exceed 100 mm (summer), 65 mm (spring and autumn), 30 mm (winter) respectively, for example, they were considered as suspicious, and they will be removed if proved wrong further by comparing the records of the adjacent stations. The method of temperature thresholds is more complex relatively. They are based on the temperature information of 20 national stations of Beijing for the past 30 years. The extreme temperature value of each month have been calculated and floating thresholds also be considered (Yang et al., 2011). For minimizing the influence of missing records on the analysis, only those sites with missing values < 3% of the total records for the 9 years are chosen for use. Additional detailed description of the methodology and quality control techniques used are accounted in details by Yang et al. (2011) and Yang and Liu (2013).

After the quality control of the data, 51 observational stations inside 6th RR are selected for use (Fig. 1) eventually, which are considered as urban observational sites. Eight reference stations surrounding the urban areas are also used in order to calculate the UHII of those urban stations. The heights of the reference stations are almost the same as those in urban areas (Table 1). Due to the importance of the selection of the reference stations, the 8 reference stations are selected by referring to a remote-sensing method as detailed in Ren and Ren (2011) and Yang et al. (2013c), which is according to a strictly defined standard, and has been confirmed objective and valid in representing rural areas in previous works (Ren and Ren, 2011; Yang et al., 2013c, 2017a).

### 2.3. Analysis methods

In the paper, UHII is estimated by calculating the temperature difference between urban and rural sites at varied time scales of hour, month, season and year. The rural temperature ( $T_r$ ) is the mean temperature values of the 8 reference stations, while the urban temperature ( $T_u$ ) is the temperature of anyone of 51 urban stations inside 6th Ring Road, or the mean values of all urban stations inside any specific urban areas. So, UHII ( $\Delta T_{u-r}$ ) can be calculated using Eq. (1)

$$UHII = \square T_{u-r} = T_u - T_r \tag{1}$$

Term Continuous Precipitation Hours of Daytime (CPHD) is applied in this study, and it is defined as the number of hours from the beginning to end of any continuous precipitation event within the periods between 0400LST and 2000 LST separately for each station

**Table 1**  
Basic information of eight reference stations.

Abbrev. (name)	Lon. (E)/Lat. (N)	Elevation (m)	Elevation difference from urban areas (m)
FHL (Fenghuangling)	116.10°/40.11°	73.0	24.6
YLD (YongleDian)	116.78°/39.68°	17.0	-31.4
PGZ (Panggezhuang)	116.34°/39.62°	34.0	-14.4
AD (Anding)	116.51°/39.62°	24.0	-24.4
NZ (Nanzhao)	116.11°/39.61°	34.0	-14.4
DXC (Dongxincheng)	116.45°/40.22°	49.0	-0.6
DSGZ (Dasungezhuang)	116.92°/40.09°	35.0	-13.4
LWT (Longwantun)	116.85°/40.23°	52.0	3.6
Average	116.51°/39.90°	31.8	-8.8

of the 51 observational sites. The hourly precipitation here is defined as rain record with  $> 0.1$  mm precipitation amount accumulated during an hour. It is further assumed that the continuous precipitation of daytime is the precipitation event that has continuous durations without any intermittence within a given period from 0400 to 2000 LST. The reason why the period of daytime precipitation is applied as an indicator is that the sunshine during daytime is one of the key factors for forming UHI phenomenon, and the sunlight-related force might be separated from those related to urban canopy geometry and anthropogenic heat release in the formation of UHI pattern, if more cases of influence of daytime precipitation on UHI could be investigated. Time period 0400LST to 2000 LST is used because the sunrise is usually around 04:30 LST and sunset around 19:30 LST in Beijing during Summer Solstice, and it thus contains the complete daytime in any months.

In order to examine the impact of varied precipitation event duration in daytime on UHI over Beijing, CPHD is further divided into four different categories, which are respectively 0 h, 0–3 h, 3–6 h and  $> 6$  h. In order to compare the differences between no-rainy case and each of the rainy cases, we also calculate UHI differences between them as following on basis of stations and regional average:

$$\Delta UHI = |UHI_{each\ rainy\ case} - UHI_{no-rainy\ case}| \quad (2)$$

There may be more than one CPHD processes in a day, especially during summertime (June to August) when  $> 70\%$  of annual total precipitation will occur in Beijing region. In this case, in order to make the analysis of UHI under different precipitation duration ranges more significant, only the event with the longest duration in a day was considered in the following calculation.

### 3. Results

#### 3.1. Characteristics of UHI and precipitation

The spatial distribution of annual mean values of UHI in the urban regions (inside the 6th RR) is shown in Fig. 2. It is obvious that the UHI spatial distribution is consistent of the divergent expansion of built-up areas and transportation system, conforming to the dense distribution of urban populations. The maximum UHI value ( $2.07^\circ\text{C}$ ) appears at Si Hui Qiao (SHQ,  $39.91^\circ\text{N}$ ,  $116.48^\circ\text{E}$ ), northeastern part inside the 4th RR. The only station with negative UHI ( $-0.25^\circ\text{C}$ ) is Dao Xiang Hu (DXH,  $40.10^\circ\text{N}$ ,  $116.18^\circ\text{E}$ ) in the northwest of the built-up areas. Previous researches have indicated that, DXH station, though inside the 6th RR, is surrounded by less buildings and a small lake nearby, which may be the reason that a negative UHI was observed (Yang et al., 2013c).

Fig. 3 shows the annual (Fig. 3a) and seasonal (Fig. 3b) mean diurnal UHI variations in urban areas over Beijing. The annual mean diurnal UHI curve contains two relatively stable stages separated by two swiftly changing stages. One stable stage is characterized by the strong UHI lasting from late evening (2100 LST) to early morning (0600 LST), and another by the weak UHI lasting from 1100 LST to 1600 LST. The rest two stages change swiftly by a drop-off (0600–1100 LST) and a surge-up (1600–2100 LST) respectively. In other inland cities, similarly stable high nocturnal UHI and weak midday UHI have also been reported (e.g. Memon et al., 2011).

Among different seasons, a common diurnal variation pattern can be found. Moreover, the length of strong stable stage in autumn (2000–0700 LST) and winter (2000–0800 LST) is a little longer than that in spring (0900–0600 LST) and summer (0900–0500 LST). Besides, for the strong stable stage, the UHI in autumn and winter are also larger than that in spring and summer. However, the stable weak stages of four seasons have relatively apparent differences. The stable weak stage in summer keeps the longest (0900–1800 LST), with the mean UHI ( $0.50^\circ\text{C}$ ) of which is higher than that of other seasons. In spring, the length of stable weak stage (1000–1700 LST) is a little shorter than that in summer, and the mean UHI is weaker ( $0.36^\circ\text{C}$ ) apparently. The stable weak stages in autumn and winter are similar in lengths (1200–1600 LST) and mean values of UHI ( $0.25^\circ\text{C}$  in autumn and  $0.34^\circ\text{C}$  in winter). It is interesting to note that though the UHI at nighttime in summer is weaker than that in other seasons, the UHI during the

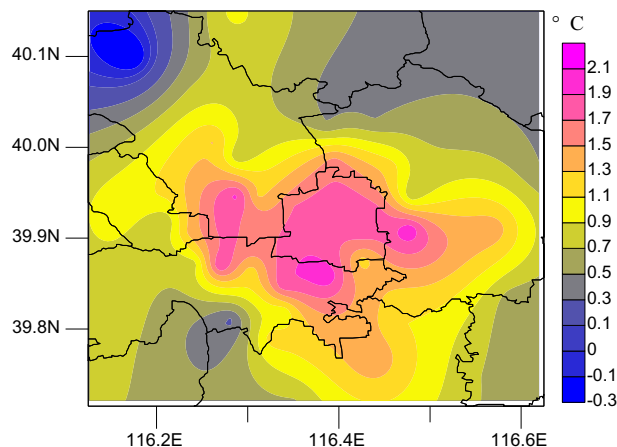


Fig. 2. Spatial distributions of annual mean values of UHI in Beijing urban area during 2007–2015.

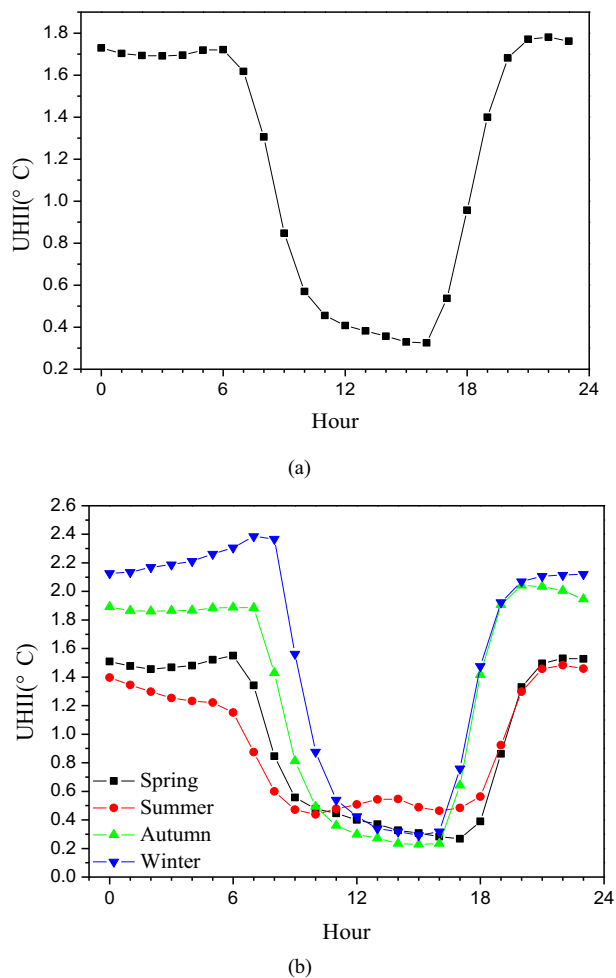


Fig. 3. Spatial distributions of UHII in (a) spring (b) summer (c) autumn (d) winter in Beijing urban area during 2007–2015.

daytime in summer is the strongest among the seasons. Similar conclusions also have been reported by Lee and Baik (2010) and Yang et al. (2013b). Roth (2007) has stated that, when rural surface is wet or saturated, thermal admittance will be increased. Thus, the daily surface temperature range will become relatively small and rural cooling during summer daytime will increase the corresponding UHII. It is also possible that the more extensive application of air conditioning in the urban areas in recent years has exaggerated the UHI effect of daytime during summer (Ren and Zhou, 2014).

The spatial distribution of annual mean occurrence times of different CPHD events during 2007–2015 is shown in Fig. 4. It is evident that the distributions of different daytime precipitation processes are rather different from each other. For no-rainy case, the lowest frequencies mainly prevail in urban center, while sites with the highest frequencies are located in the southwest to the central area. The precipitation events with  $0\text{ h} < \text{CPHD} \leq 3\text{ h}$  mostly occur in the urban center, and they occur less frequently in the western and southern parts to the urban center. For the case of  $3\text{ h} < \text{CPHD} \leq 6\text{ h}$ , the northern sites captures the highest frequencies of the precipitation events, while the fewest times come from the southeastern part of the urban areas. Meanwhile, the urban center is not characterized by the high and low centers. A more concentrated distribution in the urban center is seen for the precipitation events with  $\text{CPHD} > 6\text{ h}$ . It is therefore clear that the short duration of precipitation events ( $0\text{ h} < \text{CPHD} \leq 3\text{ h}$ ) and the long duration of precipitation events ( $\text{CPHD} > 6\text{ h}$ ) are the most basic precipitation mode over the urban center in Beijing, which is approximately in consistence to the previous study (Yang et al., 2013a).

Table 2 illustrates the significant differences among four seasons. For no-rainy days, the largest annual mean times is 85.29 in urban areas in winter, followed by 79.20 in spring, 74.86 in autumn, and 62.32 in summer. For the events of  $0\text{ h} < \text{CPHD} \leq 3\text{ h}$  and  $3\text{ h} < \text{CPHD} \leq 6\text{ h}$ , the annual mean frequencies of CPHD in whole urban areas achieve the largest values in summer. All of the times of precipitation events with  $\text{CPHD} > 6\text{ h}$  are low, being  $< 5$  times. In comparison, the frequencies of  $\text{CPHD} > 6\text{ h}$  precipitation events are the most in autumn.

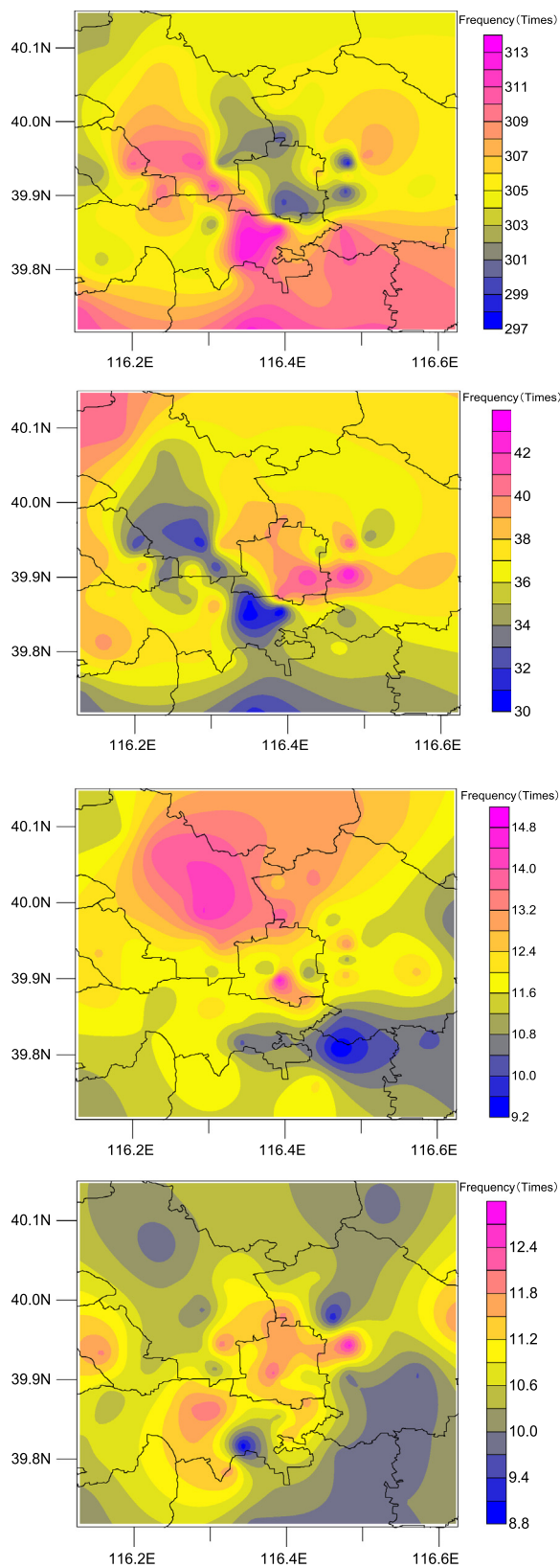


Fig. 4. Spatial distributions of frequency of CPHD with different precipitation duration ranges during 2007–2015. (a) CPHD = 0 h, (b)  $0\text{ h} < \text{CPHD} \leq 3\text{ h}$ , (c)  $3\text{ h} < \text{CPHD} \leq 6\text{ h}$ , (d)  $\text{CPHD} > 6\text{ h}$ . Unit: times.

**Table 2**

Seasonal mean frequency of CPHD in four different precipitation duration ranges over the urban areas of Beijing.

Unit (times)	CPHD = 0 h	0 h < CPHD ≤ 3 h	3 h < CPHD ≤ 6 h	CPHD > 6 h
Spring	79.20	8.49	2.28	2.03
Summer	62.32	18.09	6.13	3.69
Autumn	74.86	7.26	2.85	4.28
Winter	85.29	2.03	0.54	0.62

### 3.2. The impact of CPHD on UHII

Spatial distributions of average UHII in above four different ranges of CPHD in urban areas of Beijing during 2007–2015 are shown in Fig. 5. The spatial distributions reveal diverse features in different precipitation duration conditions. When there is no precipitation in daytime (Fig. 5a), the spatial pattern is similar to the distribution of annual mean UHII of Beijing city. This exhibits some regional differences in the effect of urbanization on surface air temperature with higher UHII in central urban area. Besides, the mean value of UHII (1.30 °C) over the whole urban areas on no-rainy days is a little higher than that on all days through whole year (1.18 °C). This is easy to understand and the similar conclusions have been found in previous researches (e.g. Hu et al., 2016). Nevertheless, noticeable discrepancies are observed in the UHII isotherm distributions in other three CPHD events (Fig. 5b–c). In the case of 0 h < CPHD ≤ 3 h (Fig. 5b), a triply weak warm cores are found in urban center and in eastern and western parts of the city near the urban center. The mean values of the warm cores are obviously lower than those in no precipitation case. For the two other precipitation duration ranges (Fig. 5c–d), the spatial differences are less significant, compared to the cases with no or less-rainy cases. Especially for the longest precipitation duration range (CPHD > 6 h), the UHII over the whole urban area is almost unable to detect.

Table 3 gives the means, maximum, minimum and range values of UHII over the urban areas in the four CPHD cases. It illustrates the significant differences among the cases. Generally speaking, the larger the CPHD, the lower the means of UHII are. In addition, the spatial difference is also closely related to the length of CPHD. It can also be seen that, the larger the CPHD is, the lower the range values of UHII are. Although the mean values of UHII warm cores are obviously lower in long duration precipitation condition than those in no precipitation, however, the UHII spatial pattern is relatively unchanged (Fig. 5), despite the average distributions of different rain events exhibit an explicit spatial difference. The higher UHII is always located in the urban centers. This may be related to the fact that, although the distributions of varied duration precipitation events are limited to a smaller extent, the cloud covers are distributed spatially broadly and consistently, leading to the uniform decline of UHII across the city.

Fig. 6 shows the diurnal variations of UHIIs in different precipitation duration ranges in Beijing city during 2007–2015. For the case of no-rainy days, the diurnal variation exhibits a typical pattern that many previous researches have shown (e.g. Lee and Baik, 2010; Yang et al., 2013c). The UHII sharply increase in the evening and decrease in the morning. Two stable stages of diurnal mean UHII could be obviously observed, a pattern similar to that shown in Fig. 4a. Compared to the case of no-rainy days, the diurnal variations of UHII with each of the rainy conditions present some different and interesting characters. Firstly, the longer the length of CPHD is, the lower the UHII will be. The diurnal character is in accordance with its spatial feature shown in Fig. 5. Secondly, the stable strong and weak stages of UHII are not apparent when the CPHD is no > 6 h, and will disappear completely when it surpasses 6 h. It means that, when precipitation events dominate the daytime, the diurnal pattern of UHII will change greatly. Thirdly, the curves of diurnal variation for two cases (3 h < CPHD ≤ 6 h and CPHD > 6 h) indicate that the UHII with serious rainy daytime (CPHD > 6 h) could be close to or a little higher than that with less rainy daytime (3 h < CPHD ≤ 6 h) for a few moments (from 1600 to 1800 LST) during the whole day. The phenomenon could not be easily explained, but may be related to the fewer samples of the CPHD > 6 h case.

The diurnal variations of seasonal mean values of UHII in different CPHD cases in Beijing city during 2007–2015 is shown in Fig. 7. All cases show clear diurnal variations in the seasonal mean UHII, with higher nighttime UHII values and lower values at noontime in different seasons. In addition, under different CPHD conditions, the mean UHII present similar diurnal variations for different seasons. For instance, stable strong or weak stages could not be found in diurnal curves of all seasons for the conditions of CPHD > 6 h, but they exist in other cases more or less. In no-rainy case, the stable strong and weak stages are longer and in deeper contrast in winter and autumn than those in spring and summer. In the case of CPHD > 6 h, the peaks of hourly UHII in different seasons all occur at midnight time with small difference. The difference of maximum (0.93 °C in spring) and minimum (0.79 °C in autumn) value is only 0.14 °C. It is notable that, under the condition of long continuous rain, the character of stronger UHI in autumn won't be kept. In addition, it is also interesting to note that the UHII varied apparently during the nighttime among the varied CPHD conditions, while the UHII differences are not so clear under different precipitation conditions during noontimes.

The average annual cycles of UHII under different precipitation conditions for 2007–2015 in urban areas of Beijing are shown in Fig. 8. The UHII has prominent seasonal characteristics. During the wet or windy season (from March to August), corresponding to spring and summer, monthly mean UHII values are lower apparently. The UHII is best developed in no-rainy case and comparably lower in each of the rainy cases. For the precipitation case of 0 h < CPHD ≤ 3 h, all of the monthly mean UHII values are lower than those of no-rainy case. In addition, the season with stronger UHII in the case of 0 h < CPHD ≤ 3 h is mostly from September to February, with the peak in December and the valley in June. Contrary to the case with no or less-rainy cases, the UHII under heavier precipitation cases of 3 h < CPHD ≤ 6 h and CPHD > 6 h has a different monthly variation. Dry seasons including winter and autumn often have higher values of UHII, but Fig. 8 shows that sometimes the UHII in wet or windy season can also reach a relatively

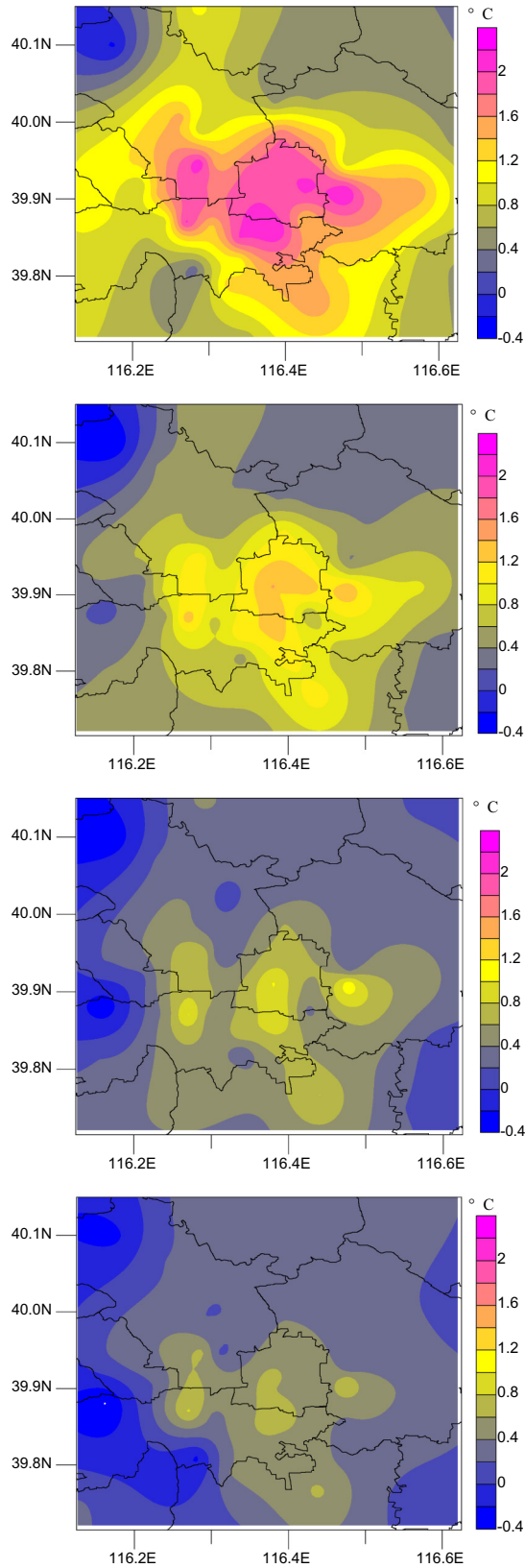


Fig. 5. Spatial distributions of UHII under different precipitation duration ranges in Beijing urban area during 2007–2015. (a) CPHD = 0 h (b)  $0\text{ h} < \text{CPHD} \leq 3\text{ h}$  (c)  $3\text{ h} < \text{CPHD} \leq 6\text{ h}$  (d)  $\text{CPHD} > 6\text{ h}$ .



**Table 3**

Means, maximum, minimum and range values of UHII over the urban areas of Beijing in four different precipitation duration ranges (Unit: °C).

	Mean	Maximum	Minimum	Range(Max-Min)
CPHD = 0 h	1.30	2.25	-0.23	2.48
0 h < CPHD ≤ 3 h	0.72	1.43	-0.38	1.81
3 h < CPHD ≤ 6 h	0.45	1.17	-0.34	1.51
CPHD > 6 h	0.36	0.84	-0.42	1.26

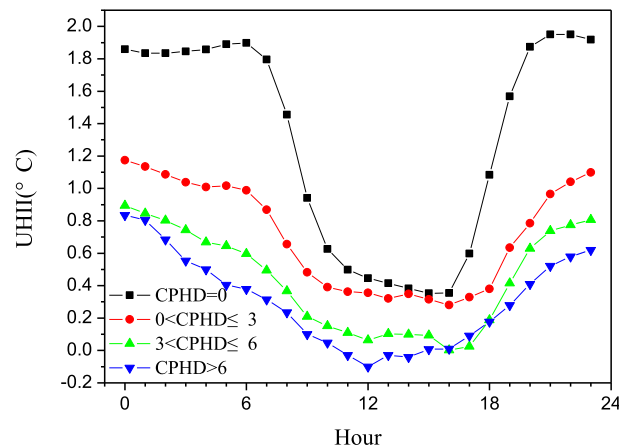


**Fig. 6.** Diurnal variations of UHII in different precipitation duration ranges in Beijing urban area during 2007–2015.

higher level. Taking the precipitation duration range of CPHD > 6 h as an example, the three lowest values of monthly mean UHII occur in July, March and April, while the UHII in May (0.36 °C) and June (0.31 °C) is not so weak, which even exceeds the monthly mean value (0.30 °C).

In order to examine their differences during different time scales, the differences of UHII in different time scale between each of the precipitation duration cases and no-rainy days have been calculated respectively, and they are shown in Figs. 9 and 10.

The lowest UHII difference in precipitation duration case of CPHD > 6 h can be found in April, May and June, and that for the case of 3 h < CPHD ≤ 6 h has a similar seasonal variation. For the case of 0 h < CPHD ≤ 3 h, however, the low ΔUHII is also found in November in addition to the similar weak periods as those in the above cases. The values of ΔUHII stay roughly at moderate levels in wet season from July to October.

In view of the diurnal variations, it is apparent that the patterns of ΔUHII in each rainy cases appears very similar (Fig. 10). The dual peak of UHII differences between each rainy case and no rainy case is close to sunrise (0600–0700 LST) and sunset (2000 LST). The minimum of ΔUHII remain stable from 1100 to 1500 LST, the period which has large solar radiation of a day. However, the differences of ΔUHII among the rainy conditions are significant. The hourly mean ΔUHII with weakest rainy condition (0 h < CPHD ≤ 3 h) have the lowest value in all of the day. The difference of hourly mean ΔUHII between the heavier (3 h < CPHD ≤ 6 h) and the heaviest (CPHD > 6 h) cases is not so prominent, however, especially for the sharply increasing and decreasing hours.

#### 4. Discussion

Many studies of urban climatology were conducted for Beijing City, and some basic features of the UHI have been evidenced (Xu et al., 2006a,b; Liu et al., 2009; Wang et al., 2011; Yang et al., 2013b). In our previous work, we have examined the detailed temporal and spatial structure of the UHII in Beijing urban areas inside the 6th RR, using the observational hourly data from 2007 to 2010 (Yang et al., 2013c). Due to the restrictions on the length of data, the previous study was concentrated merely on the general characters of UHII over Beijing urban areas. Five years later, when we do further examination of the UHII in the city in different conditions of daytime precipitation using an updated dataset, we are able to find a few of additional interesting phenomena.

It is well known that frequencies of the hourly precipitation with different types vary widely in even small urban areas, which are closely related to the surface energy and water balance. There is no doubt that the occurrence times of no-rainy days are the smallest in urban center or inside 4th RR. However, the spatial patterns of precipitation are specific for each of the different precipitation duration conditions. The spatial distribution of precipitation with 0 h < CPHD ≤ 3 h is different from that under no-rainy case with the highest values inside 4th RR. More frequencies of precipitation is not always close to the urban center, however, and this is especially true for the case of 3 h < CPHD ≤ 6 h. It seems that, when we get deep into smaller space-time scale, more complicated characters have been demonstrated, which may be due to complex structure of underlying surface and the resulting modification of surface energy balance.

A detailed spatial pattern of UHII under different types of daytime precipitation duration in the urban areas over Beijing has been

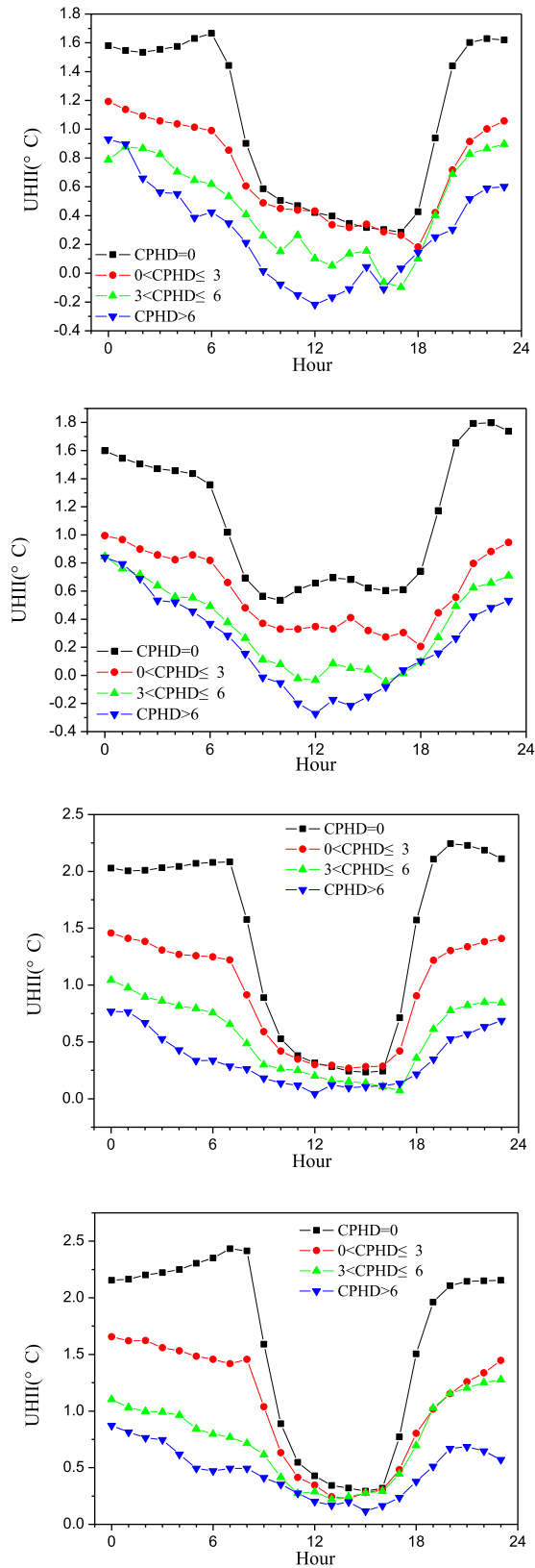


Fig. 7. Diurnal variations of seasonal mean values of UHI in different precipitation duration ranges in Beijing urban area during 2007–2015. (a) spring (b) summer (c) autumn (d) winter.

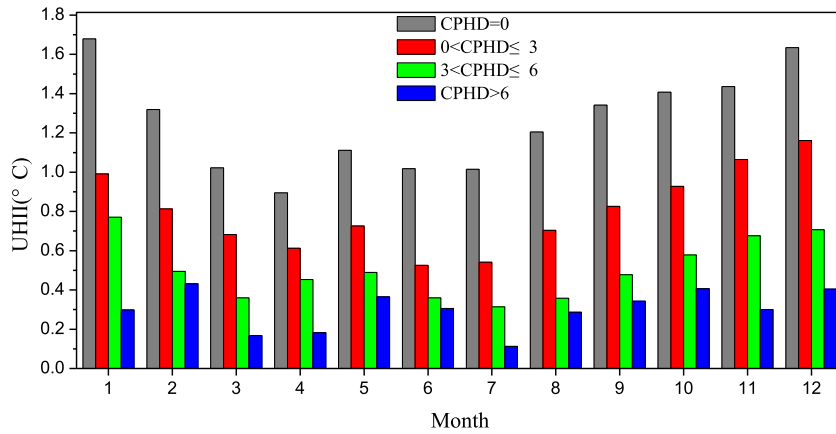


Fig. 8. Monthly mean value of UHIs in different precipitation duration ranges in Beijing urban area during 2007–2015.

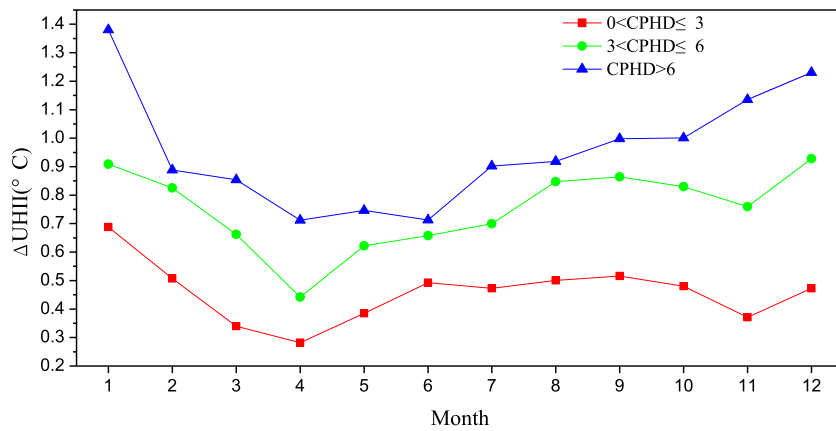


Fig. 9. Monthly variations of UHI difference between each of the precipitation duration ranges and no rainy day.

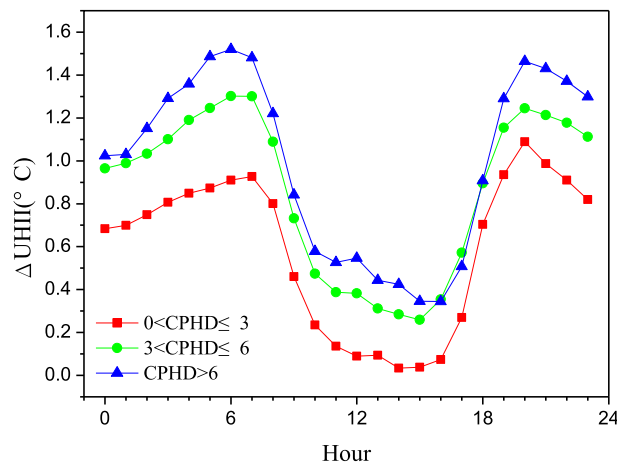


Fig. 10. Diurnal variations of UHI difference between each of the precipitation duration ranges and no rainy day.

revealed in this work. This is also the main emphasis of the analysis. It is well known that UHI is closely related to the structure, coverage, fabric, and metabolism of built-rise area, which leads to the substantial modification of surface energy and water balance (Oke, 1988). During the daytime, the multi-reflections of sunlight among high-up buildings apparently increase the absorptivity of heat in urban canopy (Ren, 2015). The reflection of urban canopy decreases, and the absorption of solar short-wave radiation and trapped heat within the urban surface therefore increase. The heat is released by long-wave radiation into sky in nighttime. The

increasing (decreasing) sensible (latent) heat flux due to the decreased soil moisture and vegetation cover is another important feature of surface energy and water balance in urban areas. Previous observations also revealed that there is difference of solar radiation and surface energy balance between city and its suburban counties (Chow and Shao, 1987).

Because of the importance of daytime solar radiation in formation and development of the UHI, we restrict the precipitation span between sunrise (0400 LST) and sunset (2000 LST), corresponding to the longest daytime on the Summer Solstice. In case of daytime precipitation, the direct solar radiation reaching at the surface is reduced to nil due to the influence of cloudiness. It is thus helpful to further recognize the contribution of direct solar radiation change to the UHI effect by examining the UHII under different durations of daytime precipitation. In daytime, when the precipitation is infrequent, the high UHII center of urban areas can still be found easily. That may be because, under weak rainy condition, the cloudiness and weather condition are not changed significantly, and the UHII is not much different from that of no-rainy condition. The heat absorbed and stored at the urban surfaces in daytime is not decreased evidently. On the contrary, under the long continuous rainy conditions, heat absorbed and stored at urban surfaces may be reduced largely owing to the lack of incoming short wave radiation, as well as the evaporation of the captured rain water at concrete surfaces. Moreover, because of the relatively high cloudiness and humidity in rainy cases, nocturnal long-wave radiative cooling is also limited. The abundant soil moisture in rural areas generally enables the rural thermal admittance to increase. Hence, the difference in thermal admittance between urban and rural areas is decreased under apparently rainy conditions, leading to a weaker UHII in the urban areas. The heavier of the rainy degree is, the more apparent the difference between rainy and no rainy cases is.

Some of previous studies on UHI and precipitation were focused on the UHI impact on precipitation event (e.g. Changnon et al., 1991; Aws et al., 2017; Yang et al., 2017c), and fewer works were turned to the opposite or the impact of precipitation on UHI. One analysis has concluded that the UHII of Beijing City reduced with an increase in precipitation levels (Liu, 2014). Although the conclusion is consistent with that reported in this paper, it was drawn based on of the limited data collected from only one station of Beijing with hourly data in only one year of 2012, and obviously needed a confirmation from a more sophisticated investigation. Our results indicated that varied precipitation durations of daytime can reduce the intensity of UHI in different extents, and this impact is more significant during nighttime. At night, the longwave radiation from the ground surface and high-rise building walls, which has been absorbed and stored in these materials during fine daytime, is emitted upward and absorbed by the near-surface atmosphere, increasing the surface air temperature and the UHII in the urban areas. If the daytime precipitation occurs continuously or frequently, the heat received and stored in the surface materials and the emission of the longwave radiation during nighttime will decreased apparently, leading to reduced surface air temperature and the UHII in the urban areas. This indicates that the solar radiation received at the urban canopy layer during daytime might have played a dominant role in the formation and variations of the UHI in Beijing City for each of the seasons.

It is found, however, that the frequency of long-duration precipitation events in winter is small. The insufficient samples may bring to some uncertainties especially for winter. The UHII spatial and temporal patterns in precipitation case with CPHD > 6 h obviously need further investigation. It is also noted that the longer period of the high-density observations, in combination with the usage of other observational data like cloudiness retrieved from satellites or radars, would greatly strengthen reliability of the analysis results.

## 5. Conclusions

In this study, the impacts of urban daytime precipitation on UHII are examined by using an hourly observational data from a high-density Automatic Weather Station (AWS) network in Beijing. The following conclusions are drawn from the analysis:

- (1) The detailed spatial distribution of precipitation over Beijing urban areas show that the short duration precipitation events ( $0 \text{ h} < \text{CPHD} \leq 3 \text{ h}$ ) and long duration precipitation events ( $\text{CPHD} > 6 \text{ h}$ ) both tend to more frequently occur over the urban center of Beijing City.
- (2) The spatial differences of UHII under different precipitation duration ranges are closely related to the length of CPHD during daytime. The longer the CPHD is, the less obvious the regional differences of UHII are and the smaller the UHII in the urban areas is.
- (3) When continuous precipitation dominates the daytime, the diurnal variation pattern of UHII will be changed greatly. The stable strong and weak stages of UHII under no-rainy condition will be not so apparent when the CPHD is larger than 0 h and < 6 h, and they will disappear completely when the CPHD surpasses 6 h.
- (4) For different types of daytime precipitation duration, the seasonal cycles of differences between each of the precipitation duration ranges and no rainy case is not similar. In the case of  $3 \text{ h} < \text{CPHD} \leq 6 \text{ h}$  and  $\text{CPHD} > 6 \text{ h}$ , the lowest UHII difference can be found in April, May and June; In the cases of  $0 \text{ h} < \text{CPHD} \leq 3 \text{ h}$ , the low  $\Delta\text{UHII}$  also occurs in November in addition to the same low-value months as those in other rainy conditions.
- (5) The diurnal variations of the differences between each of the rainy conditions and no-rainy case appeared very similar. All of them had a dual peaks close to sunrise (0600–0700 LST) and sunset (2000 LST), while the minimum value remains stable from 1100 to 1500 LST. For the sharply increasing and decreasing hours, the differences of the hourly mean  $\Delta\text{UHII}$  between the longer ( $3 \text{ h} < \text{CPHD} \leq 6 \text{ h}$ ) and the longest ( $\text{CPHD} > 6 \text{ h}$ ) cases is very small.

## Acknowledgements

The study is supported by the National Natural Science Foundation of China (Grant No. 41775078 , 41575003 and 41675092),

the Ministry of Science and Technology of China (Grant No. 2018YFA0605603).

## References

- Arnds, D., Bohner, J., Bechtel, B., 2017. Spatio-temporal variance and meteorological drivers of the urban heat island in a European city. *Theor. Appl. Climatol.* 128, 43–61. <https://doi.org/10.1007/s00704-015-1687-4>.
- Arnfield, A.J., 2003. Two decades of urban climate research: a review of turbulence, exchanges of energy and water, and the urban heat island. *Int. J. Climatol.* 23 (1), 1–26.
- Aws, A.A., Ashok, K.M., Abdul, A.K., 2017. Urban and peri-urban precipitation and air temperature trends in mega cities of the world using multiple trend analysis methods. *Theor. Appl. Climatol.* 1–16.
- Benson-Lira, V., Georgescu, M., Kaplan, S., Vivoni, E.R., 2016. Loss of a lake system in a megacity: the impact of urban expansion on seasonal meteorology in Mexico City. *J. Geophys. Res.* 121 (7), 3079–3099.
- Changnon, S.A., 1979. Rainfall changes in summer caused by St. Louis. *Science* 205, 402–404. <https://doi.org/10.1126/science.205.4404.402>.
- Changnon, S.A., Shealy, R.T., Scott, R.W., 1991. Precipitation changes in fall, winter and spring caused by St. Louis. *J. Appl. Meteorol.* 30, 126–134. [https://doi.org/10.1175/1520-0450\(1991\)030<0126:PCIFWA>2.0.CO;2](https://doi.org/10.1175/1520-0450(1991)030<0126:PCIFWA>2.0.CO;2).
- Chow, S.D., Shao, J.M., 1987. Shanghai urban influence on solar radiation. *Acta Geo. Sini.* 42, 319–327.
- Craig, K.J., Bornstein, R.D., 2002. Mm5 Simulations of Urban Induced Convective Precipitation Over Atlanta. Fourth Symp on the Urban Environment, Norfolk, VA. *Amer. Meteor. Soc.* pp. 5–6.
- Diem, J.E., Brown, D.P., 2004. Anthropogenic impacts on summer precipitation in Central Arizona. U.S.A. *Prof. Geogr.* 55, 343–355. <https://doi.org/10.1111/0033-0124.5503011>.
- Georgescu, M., Moustauoui, M., Mahalov, A., Dudhia, J., 2011. An alternative explanation of the semiarid urban area oasis effect. *J. Geophys. Res.* 116, D24113. <https://doi.org/10.1029/2011JD016720>.
- Guo, Jun, Li, Mingcai, Liu, Deyi, 2009. Effects of urbanization on air temperature of Tianjin in recent 40 years. *Ecol. Environ. Sci.* 18 (1), 29–34.
- Han, J.Y., Baik, J.J., Lee, H., 2014. Urban impacts on precipitation. *Asia-Pac. J. Atmos. Sci.* 50, 17–30. <https://doi.org/10.1007/s13143-014-0016-7>.
- Hu, X.M., Xue, M., Klein, P.M., 2016. Analysis of urban effects in Oklahoma City using a dense surface observing network. *J. Appl. Meteorol. Climatol.* 55, 723–741.
- Huff, F.A., 1986. Urban hydrometeorology review. *Bull. Amer. Meteor. Soc.* 67, 703–712.
- Kim, Y.H., Baik, J.J., 2002. Maximum urban heat island intensity in Seoul. *J. Appl. Meteorol.* 41, 651–659.
- Landsberg, H.E., 1981. *The Urban Climate*. Academic Press, New York (275pp).
- Lee, S.H., Baik, J.J., 2010. Statistical and dynamical characteristics of the urban heat island intensity in Seoul. *Theor. Appl. Climatol.* 100, 227–237. <https://doi.org/10.1007/s00704-009-0247-1>.
- Li, X.R., Hu, F., Shu, W.J., Liang, B.L., 2008. Characteristics of urban heat island effect and its meteorological influencing factors over Beijing in autumn. *Clim. Environ. Res.* 13 (3), 291–299.
- Liu, B., 2014. Temporal and Spatial Distribution Characteristics and Factor Analysis of Beijing Heat Island. Master's Thesis. Nanjing University of Information Science and Technology. Pp75.
- Liu, W.D., You, H.L., Dou, J.X., 2009. Urban-rural humidity and temperature differences in the Beijing area. *Theor. Appl. Climatol.* 96, 201–207.
- Magaña, V., Pérez, J., Méndez, M., 2003. Diagnosis and prognosis of extreme precipitation events in the Mexico city Basin. *Geofis. Int.* 42 (2), 247–260.
- Memon, R.A., Leung, D.Y.C., Liu, C.H., Leung, M.K.H., 2011. Urban heat island and its effect on the cooling and heating demands in urban and suburban areas of Hong Kong. *Theor. Appl. Climatol.* 103, 441–450. <https://doi.org/10.1007/s00704-010-0310-y>.
- Miao, S.G., Chen, F., Li, Q.C., Fan, S.Y., 2010. Impacts of urban processes and urbanization on summer precipitation: a case study of heavy rainfall in Beijing on 1 August 2006. *J. Appl. Meteorol. Climatol.* 50, 806–825. <https://doi.org/10.1175/2010JAMC2513.1>.
- Oke, T.R., 1988. The urban energy balance. *Prog. Phys. Geogr.* 12, 471–508.
- Petralli, M., Massetti, L., Orlandini, S., 2009. Solar radiation exposure of shielded air temperature sensors and measurement error evaluation in an urban environment: a preliminary study in Florence, Italy. *Adv. Sci. Res.* 3, 9–12.
- Ren, G.Y., 2015. Urbanization as a major driver of urban climate change. *Adv. Clim. Chang. Res.* 6, 1–6. <https://doi.org/10.1016/j.accre.2015.08.003>.
- Ren, Y.Y., Ren, G.Y., 2011. A remote-sensing method of selecting reference stations for evaluating urbanization effect on surface air temperature trends. *J. Clim.* 24, 3179–3189. <https://doi.org/10.1175/2010JCLI3658.1>.
- Ren, G.Y., Zhou, Y.Q., 2014. Urbanization effects on trends of extreme temperature indices of national stations over mainland China, 1961–2008. *J. Clim.* 27, 2340–2360. <https://doi.org/10.1175/JCLI-D-13-00393.1>.
- Roth, M., 2007. Review of urban climate research in (sub) tropical regions. *Int. J. Climatol.* 27, 1859–1873. <https://doi.org/10.1002/joc.1591>.
- Rozoff, C.M., Cotton, W.R., Adegoke, J.O., 2003. Simulation of St. Louis, Missouri, land use impacts on thunderstorms. *J. Appl. Meteorol.* 42, 716–738.
- Shimadera, H., Konodo, A., Shrestha, K.L., Kitaoka, K., Inoue, Y., 2015. Numerical evaluation of the impact of urbanization on summertime precipitation in Osaka. *Japan. Adv. Meteorol.* 2015, 379361.
- Song, X.M., Zhang, J.Y., AghaKouchak, A., Liu, C.S., 2014. Rapid urbanization and changes in spatiotemporal characteristics of precipitation in Beijing metropolitan area. *J. Geophys. Res. Atmos.* 119. <https://doi.org/10.1002/2014JD022084>.
- Stewart, I.D., Oke, T.R., 2012. Local Climate Zones for urban temperature studies. *Bull. Am. Meteorol. Soc.* <https://doi.org/10.1175/BAMS-D-11-00019.1>.
- Tereshchenko, I.E., Filonov, A.E., 2001. Air temperature fluctuations in Guadalajara, Mexico, from 1926 to 1994 in relation to urban growth. *Int. J. Climatol.* 21, 483–494.
- Thielen, J., Wobrock, W., Gadian, A., Mestayer, P.G., Creutin, J.D., 2000. The possible influence of urban surfaces on rainfall development: a sensitivity study in 2D in the meso- $\gamma$ -scale. *Atmos. Res.* 54, 15–39.
- Wang, J.P., Sun, J.S., Wang, S.G., 2011. Impact of basin terrain urban Heat Island effect on precipitation in surrounding region of Xi'an. *J. Arid Meteorol.* 29 (2), 168–173.
- Wang, Q.C., Guo, L.P., Zhang, S.H., 2019. Urban heat island effect under different meteorological conditions over Langfang Hebei province. *J. Meteorol. Environ.* 25 (6), 44–48.
- Xu, X.D., Ding, G.A., Bian, L.G., 2006a. Beijing city air pollution observation experiment. *J. Appl. Meteorol. Sci.* 17 (6), 815–828.
- Xu, Z., Zhang, L., Ruan, B., 2006b. Analysis on the spatiotemporal distribution of precipitation in the Beijing region. *Arid Land Geogr.* 29 (2), 186–192.
- Yang, P., Liu, W.D., 2013. Evaluating the quality of meteorological data measured at automatic weather stations in Beijing during 1998–2010. *Adv. Meteorol. Sci. Technol.* 3, 27–34.
- Yang, P., Liu, W.D., Zhong, J.Q., Yang, J., 2011. Evaluating the quality of temperature measured at automatic weather stations in Beijing. *J. Appl. Meteorol. Sci.* 22, 706–715.
- Yang, P., Ren, G.Y., Hou, W., Liu, W.D., 2013b. Spatial and diurnal characteristics of summer rainfall over Beijing municipality based on a high-density AWS dataset. *Int. J. Climatol.* 33, 2769–2780. <https://doi.org/10.1002/joc.3622>.
- Yang, P., Ren, G.Y., Liu, W.D., 2013c. Spatial and temporal characteristics of Beijing urban heat island intensity. *J. Appl. Meteorol. Climatol.* 52, 1803–1816. <https://doi.org/10.1175/JAMC-D-12-0125.1>.
- Yang, P., Ren, G.Y., Yan, P.C., 2017a. Evidence for a strong association of short-duration intense rainfall with urbanization in the Beijing urban area. *J. Clim.* 30, 5851–5870. <https://doi.org/10.1175/JCLI-D-16-0671.1>.
- Yang, P., Ren, G.Y., Hou, W., 2017b. Temporal-spatial patterns of relative humidity and the urban dryness island effect in Beijing city. *J. Appl. Meteorol. Climatol.* <https://doi.org/10.1175/JAMC-D-16-0338.1>.
- Yang, P., Xiao, Z.N., Shi, W.J., 2017c. Fine-scale characteristics of rainfall in Beijing urban area based on a high-density AWS dataset. *Chin. J. Atmos. Sci.* 41 (3), 475–489.
- Zhao, Lei, Lee, Xuhui, Smith, Ronald B., Oleson, Keith, 2014. Strong contributions of local background climate to urban heat islands. *Nature* 511 (10), 216–219. <https://doi.org/10.1038/nature13462>.
- Zhong, S., Qian, Y., Zhao, C., Leung, R., Yang, X.Q., 2015. A case study of urbanization impact on summer precipitation in the greater Beijing metropolitan area. urban heat island versus aerosol effects. *J. Geophys. Res. Atmos.* 120, 10903–10914. <https://doi.org/10.1002/2015JD023753>.
- Zhou, Decheng, Zhao, Shuqing, Zhang, Liangxia, Sun, Ge, Liu, Yongqiang, 2015. The footprint of urban heat island effect in China. *Sci. Rep.* 5, srep11160. <https://doi.org/10.1038/srep11160>.